Published in final edited form as:
Phys Chem Chem Phys. 2015 December 21; 17(47): 31653–31661. doi:10.1039/c5cp05873b.

Contact angles and wettability of ionic liquids on polar and non-polar surfaces†

Matheus M. Pereira[#a], **Kiki A. Kurnia**[#a,b], **Filipa L. Sousa**[a], **Nuno J. O. Silva**[c], **José A. Lopes-da-Silva**[d], **João A. P. Coutinho**[a], and **Mara G. Freire**[a,*]

[a]CICECO – Aveiro Institute of Materials, Department of Chemistry, University of Aveiro, 3810-193 Aveiro, Portugal

[b]Center of Research in Ionic Liquids, Department of Chemical Engineering, Universiti Teknologi PETRONAS, Bandar Seri Iskandar, 32610 Perak, Malaysia

[c]CICECO – Aveiro Institute of Materials, Departamento de Física, Universidade de Aveiro, 3810-193 Aveiro, Portugal

[d]QOPNA Unit, Department of Chemistry, Universidade de Aveiro, 3810-193 Aveiro, Portugal

[#] These authors contributed equally to this work.

Abstract

Many applications involving ionic liquids (ILs) require the knowledge of their interfacial behaviour, such as wettability and adhesion. In this context, herein, two approaches were combined aiming at understanding the impact of the IL chemical structures on their wettability on both polar and non-polar surfaces, namely: (i) the experimental determination of the contact angles of a broad range of ILs (covering a wide number of anions of variable polarity, cations, and cation alkyl side chain lengths) on polar and non-polar solid substrates (glass, Al-plate, and poly-(tetrafluoroethylene) (PTFE)); and (ii) the correlation of the experimental contact angles with the cation–anion pair interaction energies generated by the Conductor-like Screening Model for Real Solvents (COSMO-RS). The combined results reveal that the hydrogen-bond basicity of ILs, and thus the IL anion, plays a major role through their wettability on both polar and non-polar surfaces. The increase of the IL hydrogen-bond accepting ability leads to an improved wettability of more polar surfaces (lower contact angles) while the opposite trend is observed on non-polar surfaces. The cation nature and alkyl side chain lengths have however a smaller impact on the wetting ability of ILs. Linear correlations were found between the experimental contact angles and the cation–anion hydrogen-bonding and cation ring energies, estimated using COSMO-RS, suggesting that these features primarily control the wetting ability of ILs. Furthermore, two-descriptor correlations are proposed here to predict the contact angles of a wide variety of ILs on glass, Al-plate, and PTFE surfaces. A new extended list is provided for the contact angles of ILs on three surfaces, which can be used as *a priori* information to choose appropriate ILs before a given application.

maragfreire@ua.pt; Fax: +351-234-370084; Tel: +351-234-401422.

Europe PMC Funders Author Manuscripts

Introduction

In recent decades, ionic liquids (ILs) have attracted significant attention as neoteric solvents for chemical reactions and separation processes due to their remarkable properties, such as non-volatility, negligible vapour pressure, and high thermal and chemical stabilities.1 Nonetheless, the most fascinating feature arises from the possibility of tuning their physicochemical properties by simply varying their constituting ions,2 so that an IL with desirable properties can be designed for a specific application. As a result, ILs have been studied as alternative media for numerous applications.3–5 For applications involving ILs in heterogeneous systems and transport in capillary, fibrous, or porous environments, their interfacial properties, such as surface/interfacial tension and wettability (the tendency of a fluid to spread on a given solid surface that may be estimated by the measurement of the contact angle), have to be known. Although some attention has been devoted to the surface tension of pure ILs and their mixtures with molecular solvents,6 the determination of contact angles of ILs on solid surfaces, aiming at characterizing their wettability, has received limited attention.7–13 Gao and McCarthy8 reported the wettability of four ILs on various hydrophobic and super-hydrophobic surfaces, and highlighted a significant complex analysis of the contact angles of ILs since both ions of the probe liquid can interact with the surfaces evaluated. Restolho *et al.*9–12 and Carrera *et al.*13 described the wetting behaviour of ILs as a main result of their dispersive and non-dispersive interactions with the solid substrate. Other researchers14–18 turned to electrowetting studies aiming at enhancing wettability by applying an external voltage across the solid–liquid interface. While all these studies7–18 contribute to the understanding of the wetting phenomenon, there are still few ILs investigated resulting in the lack of a comprehensive analysis of the impact of the chemical structures of ILs and their wetting behaviour.

A fundamental understanding of the relationship between the chemical structures of ILs and wettability is of crucial relevance envisaging a rational synthesis and design of ILs for a specific task, particularly when taking into consideration the large number of possible ILs that can be synthesized. The studies being carried out by us have been focused on combining experimental and theoretical or computational-based approaches aiming at identifying promising IL candidates for specific purposes before carrying out extensive and trial-and-error experimental measurements. In previous studies, we have established the connection between the chemical structures of ILs and their mutual solubilities with water.19–27 More recently, we have correlated the hydrogen-bond acceptor and donor abilities of ILs with the IL cation–anion interaction energies, allowing us to propose extended basicity28 and acidity29 scales for ILs. Furthermore, based on computational approaches, we have designed and proposed three potential novel ILs to be used as absorbents in absorption-refrigeration systems,30 and have also identified promising ILs for the desulfurization of fuels,31 and for the extraction of ethanol in IL–water mixtures.32 These studies show how the fundamental knowledge of structure–property relationships of ILs allows their adequate design to meet the requirements of a target application.

Herein, aiming at understanding the impact of the chemical structures of ILs on their wetting ability on both polar and non-polar surfaces, the contact angles of a broad range of ILs, comprising a wide selection of cations, anions and cation alkyl side chain lengths, were

experimentally determined. The novel experimental data for a large variety of ILs were then interpreted and discussed taking into account their chemical structures. The contact angle data were subsequently correlated with the interaction energies of the IL cation–anion pairs generated by the Conductor-like Screening Model for Real Solvent (COSMO-RS).33,34 Based on their linear dependence, an extended list for the wettability of 480 ILs in 3 surfaces is proposed here.

Results and discussion

Contact angle measurements

The experimental contact angle values at 298.2 K for the ILs investigated in this work are reported in Table 1. A comparison with literature data is challenging due to lack of values for the same surfaces. Nevertheless, a good agreement is observed between the data measured in this work and those previously published by Carrera *et al.*13 In particular, the contact angles of $[C_4C_1im][NTf_2]$ ($\theta = 66.25°$)13 and $[C_4C_1im][N(CN)_2]$ ($\theta = 81.71°$)13 on PTFE are in close agreement with the values obtained in this work. On the other hand, the same authors13 reported a much higher contact angle of $[C_4C_1im][BF_4]$ ($\theta = 81.71°$) on PTFE than the value measured here (65.07°). Batchelor *et al.*35 and Restolho *et al.*9 also reported the contact angle of $[C_4C_1im][BF_4]$ on the same surface, and their values were 79° and 95°, respectively. This disagreement in contact angle values could be a result of the different IL samples used and their respective purity level and/or water content. Indeed, Freire *et al.*36 have demonstrated that $[C_4C_1im][BF_4]$, in the presence of water, is not stable and has a high tendency to suffer hydrolysis. Therefore, the chemical stability of $[C_4C_1im][BF_4]$ (either in our samples or those used by other authors) should be behind the differences reported. Even so, given the fluorinated nature of the IL anion and of the PTFE surface, low contact angles are expected for $[C_4C_1im][BF_4]$.

The data presented in Table 1 show that, for the same IL, the contact angles on the glass and Al-plate surfaces are lower than on PTFE, and follow the trend: glass < Al-plate < PTFE. In general, the glass and Al-plate surfaces are easier to wet by more hydrophilic ILs or with a higher hydrogen-bond basicity, such as $[C_4C_1im][Ac]$ and $[C_4C_1im][DMP]$.28 In the glass surface, the presence of surface hydroxyl groups should be responsible for the improved wetting behaviour. Using molecular dynamics simulations, Cione *et al.*37 have shown that the interactions between the –OH groups on the glass surface and the IL ions decrease the strength of the cation–anion interactions, further inducing a decrease in the local surface tension and, consequently, improving the wetting ability of ILs. On the other hand, higher contact angle values were observed for the PTFE surface, and that can be attributed to the chemical structure/nature of the organofluoride polymer. Even so, ILs with fluorinated anions display lower contact angles on the PTFE surface than those composed of non-fluorinated anions. In this polymer, the carbon atoms are linked to electronegative and repulsive fluorine atoms minimizing thus the interactions of ILs with PTFE.38 These results reveal significant wettability differences of ILs on polar and non-polar surfaces where, on the whole, ILs have a higher affinity to wet polar surfaces – a direct outcome of their remarkable hydrogen-bonding ability as discussed below.

The wide range of ILs studied in this work allows investigating the impact of the structural variations of ILs, namely the anion and cation nature, as well as the cation alkyl side chain length, on their wetting ability of polar and non-polar surfaces. By changing the IL anion, the contact angle values vary significantly on glass surfaces – from 20.63° for $[C_4C_1im][Ac]$ to 52.46° for $[C_4C_1im][PF_6]$. The glass surface is easier to wet by the polar $[C_4C_1im][Ac]$ rather than using the more hydrophobic $[C_4C_1im][PF_6]$. For $[C_4C_1im]$-based ILs, anions can be ranked based on increasing contact angles in the glass surface as follows: $[Ac]^- < [DMP]^- < [TFA]^- < [N(CN)_2]^- < [EtSO_4]^- < [MeSO_4]^- < [CF_3SO_3]^- < [SCN]^- < [C(CN)_3]^- < [NTf_2]^- < [BF_4]^- < [PF_6]^-$. This rank of anions closely follows the extended basicity scale of $[C_4C_1im]$-based ILs proposed by Cláudio *et al.*28 Generally, the higher the anion hydrogen-bond basicity, *i.e.*, the ability of the IL anion to accept protons, the easier it is for the IL to wet the polar glass surface. A similar rank of anions to wet the polar Al-plate surface was observed (and in a slightly more expanded range of contact angle values). This phenomenon might be linked to the chemical structure of the aluminium plate surface. Anwander *et al.*39 suggested the presence of surface coordination of aluminium atoms in monomeric or oligomeric forms, in particular the presence of highly acidic and reactive tri-coordinated Al(III) species. This “acidic” Al-plate surface has a high affinity for ILs with high basicity and, ultimately, the surface is easier to wet using ILs of higher hydrogen-bond basicity. In summary, for polar glass and Al-plate surfaces, the hydrogen bonding ability of the anion plays a dominant role in the wetting ability of ILs – the higher the hydrogen-bond basicity of ILs the easier is to wet the polar surfaces.

On the other hand, a reverse rank of the anions to wet the non-polar PTFE surface was observed; an increase in the IL hydrogen-bond basicity leads to higher contact angles, and thus to a decreased ability to wet this surface. The same anion trend was observed by Carrera *et al.*13 While these authors13 studied a more limited number of ILs, they showed the higher aptitude of low basicity ILs, such as $[C_4C_1im][NTf_2]$, to wet the non-polar PTFE surface when compared to ILs with higher basicity, *e.g.*, $[C_4C_1im][N(CN)_2]$. In addition, the same rank of anions to wet the non-polar PTFE surface was also observed when some of these anions are combined with other cations, namely methyltrioctylammonium.13 Li and co-workers,40 using 6 ILs, also revealed that ILs with lower hydrogen-bond basicity have a higher ability to wet the non-polar PTFE surface.

Based on the results obtained here for an extended number of $[C_4C_1im]$-based ILs, and other literature values previously reported,13,40 it is clear that the hydrogen-bond basicity of the IL anion plays a dominant role in the wettability of ILs, either on polar or non-polar surfaces. On polar surfaces the wettability of ILs increases with their hydrogen-bond basicity, whereas the opposite effect is observed for non-polar surfaces.

While the contact angle values significantly differ with the IL anion, the same was not observed with the IL cation head group and alkyl side chain length. For instance, increasing the alkyl side chain length from $[C_2C_1im][NTf_2]$ to $[C_9C_1im][NTf_2]$ results in a small increase of the contact angle on the glass surface, from 37.66° to 46.11°. A similar trend was observed with the Al-plate surface. Cations with short alkyl side chains are slightly more suitable to wet polar surfaces, as expected, owing to the higher hydrophobicity as the size of the alkyl chain increases. As observed previously with the IL anion effect, a reversed trend

Europe PMC Funders Author Manuscripts

on the wettability is observed for the non-polar PTFE surface. Furthermore, for ILs with the same anion and longer alkyl side chains, the contact angle values become increasingly more similar amongst the several surfaces since the hydrogen-bonding interactions become less significant.

The results reported in Table 1 indicate that the IL anion plays the primary role in their wetting capacity, thus being a consequence of their hydrogen-bonding ability and ability to interact with each polar and non-polar surface, whereas the cation alkyl side chain length and the cation head group display a less significant and secondary effect. Nevertheless, it should be highlighted that they can also be used to adjust the wetting ability of ILs although in a narrower extent.

COSMO-RS

Aiming at gathering a deeper insight into the mechanisms that control the wettability of ILs on polar and non-polar surfaces, as well as to attempt the development of a predictive model able to estimate *a priori* contact angle values that would help in the design of new ILs, COSMO-RS was used herein.

From COSMO-RS calculations, three cation–anion interaction energies, namely electrostatic/misfit, E_{MF}, hydrogen-bonding, E_{HB}, and van der Waals forces, E_{vdW}, can be estimated (plus the total interaction energy, E_{INT}). These energy descriptors generated by COSMO-RS have been successfully used to describe the hydrogen-bond basicity28 and acidity29 of ILs, as well as the adsorption ability of ILs and chlorinated compounds onto carbon surfaces.41–43 In addition to those descriptors, here we introduced an additional descriptor, the ring correction energy, E_{Ring}. The E_{INT}, E_{MF}, E_{HB}, E_{vdW}, and E_{Ring} values for the studied ILs are given in Table S1 in the ESI.† These five descriptors allowed us to develop a model to predict IL contact angles on both polar and non-polar surfaces.

In order to select proper descriptors able to describe contact angles of ILs on the different surfaces, a stepwise regression method was used. In this way, a stepwise model-building approach was addressed, starting with a single descriptor variable for the identification of an initial model. Then, the model was repeatedly improved from the previous step by adding (forward stepwise) or removing (back stepwise) a new variable, while the stepwise approach stopped when no further improvements in the model were observed. The best single predictor for each correlation, initially selected according to the highest correlation coefficient obtained, was used for the initial linear regression step. As a next step, one descriptor was added at a time, always adding the one that improves the description, until no longer significant improvements were observed. The final regression equation was achieved when the significant variables were identified.

As an initial step to develop a correlation between the wettability of ILs on the glass surface, as well as to infer on their possible dependence on cation–anion interaction energies, we correlated the experimental contact angle values acquired in this work as a function of individual descriptors. The accuracy of the correlations was ascertained by the correlation coefficient, R^2, the Fisher significance parameter (a statistical significance test used in the analysis of contingency tables), F, and the average absolute relative deviation (AARD). The

AARD was calculated using the equation given in the ESI.† The correlations that describe the one-descriptor models for the contact angles of ILs on the glass surface are given by eqn (1) in Table 2 (and eqn (S1) to (S4) in Table S2 in the ESI†) along with their statistical parameters. The one-descriptor parameter equations, using only E_{INT}, E_{MF}, E_{vdW}, or E_{Ring}, yield poor R^2 and F, and high AARD values, and thus these are not statistically relevant in the description of the contact angles of ILs onto the glass surface. Additional information on these equations can be found in Table S2 in the ESI.† In summary, electrostatic and dispersive interactions have no significant impact on the contact angle, and consequently, on the wetting ability of ILs on polar glass surfaces. The correlation using E_{HB} produced the highest R^2 and F, and lower AARD values when compared to the other one-descriptor correlations. This is a clear indication that the cation–anion hydrogen-bond energies of ILs reflect the hydrogen-bonding ability of their ions to interact with the glass surface, and thus, their wetting ability. In this way, ILs with higher cation–anion interaction energies show an improved ability to wet the polar glass surface. This is in agreement with the contact angle dependence of the hydrogen-bonding basicity of ILs discussed before. Thus, it can be concluded that, among the three specific cation–anion interaction energies, hydrogen-bond plays a dominant role in their wettability on polar surfaces.

Although a reasonable one-descriptor correlation using E_{HB} can be proposed for the glass surface, this model only yields a R^2 of 0.8005 and a F value of 101.2492 (*cf.* eqn (1) in Table 2). As such, even though eqn (1) might be useful for predicting the contact angles of ILs with similar chemical structures to those used in the dataset, higher R^2 and F values are expected aiming at gathering more detailed molecular-level information on the wetting behaviour of ILs as well as to display some predictive ability for other ILs not used in the correlation development. For that purpose, the correlation of the measured contact angles using a multi-descriptor approach was attempted. Since the E_{HB} was found to play a dominant role, extra descriptors were further added to eqn (1) resulting in a series of equations listed in Table 2 (and eqn (S5)–(S10) in Table S2 in the ESI†). It should be noted that E_{INT} is not included in the development of multi-descriptor correlations as it does not represent any specific type of interaction. Adding E_{MF} or E_{vdW} to eqn (1) leads to correlations with similar R^2 and F values (*cf.* eqn (S5) and (S6) in Table S2 in the ESI†) and thus, these two-descriptor correlations are not statistically significant. Curiously, the combination of E_{MF} and E_{vdW} (*cf.* eqn (S7) in Table S2 in the ESI†) gives a correlation with R^2 and F values lower than eqn (1) and, therefore, further confirming that electrostatic/misfit interactions and van der Waals forces do not have a significant contribution towards the wetting ability of ILs. Significant improvements in the R^2 and F values, 0.9117 and 130.1319, respectively, can be achieved by combining E_{HB} and E_{Ring} (*cf.* eqn (2) in Table 2) which is an indication that the contact angles of ILs on polar glass surfaces are not only controlled by hydrogen-bonding interactions, but also by the ring energy, which depends on the number of atoms forming the ring, and thus on the IL size and steric effects. Nevertheless, it should be taken into account that the presence of cyclic cations can also influence the cation–anion cohesive energy and further the ability of the IL anion to interact with each surface.

The same type of approach was applied for the correlation of the contact angles of ILs on the Al-plate surface (*cf.* eqn (3) and (4) in Table 2, and eqn (S11)–(S20) in Table S3 in the

ESI†). Similar trends were observed, in which an evaluation of the best models identifies the hydrogen-bond interaction energy descriptor, E_{HB}, as the most statistically significant. Even so, the one-descriptor model using E_{HB} to correlate the contact angles on the polar Al-plate produces higher R^2 and F values (*cf.* eqn (3) in Table 2) than on the glass surface. This observation may indicate that the hydrogen-bonding of the IL ions with the Al-surface is more relevant than that observed in the glass surface where the size of the cation ring also played a role. However, the E_{Ring} also has a secondary influence on the wetting behaviour of ILs onto the Al-plate since higher R^2 and F values were obtained when including this descriptor.

A similar procedure was applied for the correlation of the contact angles of ILs in the PTFE surface. Unlike the glass and Al-plate, the PTFE surface is non-polar. Nevertheless, the correlations obtained (*cf.* eqn (5) and (6), and eqn (S21)–(S30) in Table S4 in the ESI†) reveal that the hydrogen-bonding interactions of the cation–anion pairs also play a dominant role in the contact angle, and subsequently, in the wetting ability of ILs on the non-polar PTFE surface, albeit in an opposite trend to that observed with the polar surfaces (as denoted by the negative values of the coefficients in the equations corresponding to PTFE). The stronger the hydrogen-bond strength of the IL ions pairs, the lower their interaction with the PTFE surface (supported by high contact angle values). Similar to the correlations obtained for the polar surfaces, the two-descriptor correlations which contain hydrogen-bonding and cation ring size energies prove to be the most statistically significant.

In summary, the contact angles of a large number of ILs on polar and non-polar surfaces can be described by a fixed set of quantum-derived parameters, namely by IL cation–anion interaction energies. Eqn (2), (4), and (6) were then used to estimate the θ values of neat ILs (the comparison using other equations is given in Fig. S1–S30 in the ESI†). Fig. 1 depicts the relationship between the experimental and estimated θ parameters. There is a close agreement between the experimental and predicted θ meaning that eqn (2), (4), and (6) can thus be used to predict the contact angles of a wide variety of ILs with reasonable accuracy. These three equations were constructed using a broad range of chemically different ILs, comprising imidazolium-, piperidinium-, and pyridinium cations, anions of almost extreme hydrogen-bond basicity ($[C_4C_1im][DMP] = 1.12$ *versus* $[C_4C_1im][PF_6] = 0.21$),28,44 and with cations with variable alkyl side chain length. Correlations with high R^2 and F values were obtained further validating the use of the *a priori* cation–anion interaction energy descriptors for the prediction of the contact angles of ILs on both polar glass and Al-plate and on the non-polar PTFE surfaces.

In recent years, significant progress has been made in identifying structure-related descriptors aiming at describing the physicochemical properties of ILs, such as density,45 polarity,46 basicity/acidity,28 and toxicity.47 However, there still lacks a databank or predictive methods for the contact angles of ILs on both polar and non-polar surfaces. Driven by the prediction results presented above, eqn (2), (4), and (6) were then used to predict the contact angles of other ILs not studied in this work (or ILs with no experimental data yet available). A database of contact angles of ILs on polar and non-polar surfaces comprising 10 1-alkyl-3-methylimidazolium-based cations (this set of cations was chosen because these are the most studied ILs so far) combined with 48 anions of different

hydrogen-bond basicity, resulting in a total of 480 ILs, was finally built. This novel data set contains ILs with similar structures in the database, such as ILs with propanoate ([Pro]$^-$), butanoate ([But]$^-$) and hexanoate ([Hex]$^-$) which have similar structures to [Ac]– and that is used in the training dataset. For other ILs, none or similar anions are present in the experimental data set, such as tris(pentafluoroethyl)-trifluorophosphate, [eFAP]; and tris(nonafluorobutyl)trifluorophosphate, [bFAP]. In general, the extent of this database can be as large as desired since the correlation methods developed only require cation–anion interaction energies that can be estimated using COSMO-RS. The full name, abbreviation, and cation or anion numbering of ILs, along with their cation–anion interaction energy descriptors, are given in Table S5 in the ESI.† The predicted θ values on polar and non-polar surfaces are given in Table S6 in the ESI,† and depicted in Fig. 2.

In general, ILs composed of hydrogensulphate or carboxylate-based anions (anions number 1 to 6, for full anion number see Table S5 in the ESI†) display low contact angles regardless of the cation alkyl chain length. In contrast, these ILs display high contact angles on the non-polar PTFE surface. It is also note-worthy to mention that ILs with a low hydrogen-bond basicity anion, such as [eFAP]– and [bFAP]–, show high contact angles on the glass and Al-plate surfaces, while presenting low contact angles on the PTFE surface. The predicted contact angles reinforce the idea that while the IL anion has a significant influence on their wetting ability, the cation core and the alkyl chain length only present a slight contribution. For instance, the predicted contact angles in the glass surface just varied from 17.18° to 19.91° for [C_1C_1im][Ac] to [$C_{10}C_1$im][Ac]. These structural variations may, however, be used to fine-tune the physical properties of ILs to meet the requirements of a task-specific application. In summary, Fig. 2 depicts the prediction of the contact angles of 480 ILs in 3 surfaces that can be used as *a priori* information before extensive and experimental trial-and-error approaches.

Conclusions

In this work, a comprehensive investigation on the impact of the chemical structures of ILs (cation head group, anion nature, and cation alkyl side chain length) on their wettability of polar and non-polar surfaces was carried out through the experimental measurements of contact angles. The gathered results, at least considering the families of ILs investigated in this work, demonstrate that the hydrogen-bonding ability of ions plays a dominant role – the increase of the hydrogen-bond basicity of the ILs increases their ability to wet polar surfaces whereas it reduces their capability to wet non-polar ones.

In order to further develop predictive correlations for the contact angles of ILs, the set of experimental data obtained here was correlated with cation–anion interaction energies generated using COSMO-RS, a quantum chemical-based prediction model. The high correlation coefficients and Fisher significance parameters obtained validated the *a priori* cation–anion interaction energy descriptors for the prediction of the IL contact angles. Accordingly, two-descriptor correlations were proposed to predict the contact angles of ILs on the polar glass and Al-plate surfaces as well as on the non-polar PTFE surface. These correlations may be valuable for the design and applications of a target IL with pre-defined

wettability. A final databank comprising the contact angles of 480 ILs on 3 surfaces was proposed here.

Materials and methods

Materials

A broad range of ILs was studied in this work in order to evaluate the impact of their chemical structures, namely the cation core, the anion nature, and the cation alkyl side chain length, on the contact angles of ILs on both polar and non-polar surfaces. The ILs investigated were: 1-butyl-3-methylimidazolium acetate, [C_4C_1im][Ac]; 1-butyl-3-methylimidazolium dimethylphosphate, [C_4C_1im][DMP]; 1-butyl-3-methylimidazolium trifluoroacetate, [C_4C_1im][TFA]; 1-butyl-3-methylimidazolium dicyanamide, [C_4C_1im][$N(CN)_2$]; 1-butyl-3-methylimidazolium ethylsulphate, [C_4C_1im][$EtSO_4$]; 1-butyl-3-methylimidazolium methylsulphate, [C_4C_1im][$MeSO_4$]; 1-butyl-3-methylimidazolium trifluoromethanesulfonate, [C_4C_1im][CF_3SO_3]; 1-butyl-3-methylimidazolium thiocyanate, [C_4C_1im][SCN]; 1-butyl-3-methylimidazolium tricyanomethane, [C_4C_1im][$C(CN)_3$]; 1-butyl-3-methylimidazolium tetrafluoroborate, [C_4C_1im][BF_4]; 1-butyl-3-methylimidazolium hexafluorophosphate, [C_4C_1im][PF_6]; 1-butyl-3-methylimidazolium bis(trifluoromethylsulfonyl)imide, [C_4C_1im][NTf_2]; 1-ethyl-3-methylimidazolium bis(trifluoromethylsulfonyl)imide, [C_2C_1im][NTf_2]; 1-methyl-3-propylimidazolium bis(trifluoromethylsulfonyl)imide, [C_3C_1im][NTf_2]; 1-methyl-3-pentylimidazolium bis(trifluoromethylsulfonyl)imide, [C_5C_1im][NTf_2]; 1-hexyl-3-methylimidazolium bis(trifluoromethylsulfonyl)imide, [C_6C_1im]-[NTf_2]; 1-heptyl-3-methylimidazolium bis(trifluoromethylsulfonyl)imide, [C_7C_1im][NTf_2]; 1-methyl-3-octylimidazolium bis(trifluoromethylsulfonyl)imide, [C_8C_1im][NTf_2]; 1-methyl-3-nonylimidazolium bis(trifluoromethylsulfonyl)imide, [C_9C_1im][NTf_2]; 1-methyl-1-propylpiperidinium bis(trifluoromethylsulfonyl)imide, [C_3C_1pip][NTf_2]; 1-butyl-1-methylpiperidinium bis(trifluoromethylsulfonyl)imide, [C_4C_1pip][NTf_2]; and 1-butyl-3-methylpyridinium bis(trifluoromethylsulfonyl)imide, [C_4C_1py][NTf_2]. The chemical structures of the ions of the ILs investigated are given in Fig. 3. These ILs were purchased from Iolitec with a purity level higher than 98 wt%. Prior to the measurements of contact angles, individual samples of each IL were dried under constant agitation and vacuum (10^{-2} Pa) at 323 K for at least 48 h in order to remove traces of water and volatile compounds. After this procedure, the purity of each IL was further checked using ^{1}H, ^{13}C, and ^{19}F (whenever possible) NMR spectroscopy.

The solid substrates studied were poly-(tetrafluoroethylene) (PTFE) with 1 mm thickness (Goodfellow), Al-plate (Extrusal) and optical quality glass (VWR). The substrates were carefully cleaned with a detergent solution, rinsed several times with distilled and deionized water, dried with nitrogen and for 2 h inside a vacuum oven at room temperature.

Contact angle measurements

Contact angle measurements were carried out using the sessile drop method with the Contact Angle System OCA 20 (Data-Physics Instruments GmbH, Germany) at 298.2 K. Drop volumes of (12 ± 1) mL were obtained using a Hamilton DS 500/GT syringe connected to a

Europe PMC Funders Author Manuscripts

Teflon coated needle placed inside an aluminium chamber able to maintain the temperature of interest within ±0.1 K. The contact angle evolution over time was recorded, for time intervals ranging from 10 to 60 min, depending on the liquid spreading kinetics. When a plateau was achieved, the so-called static contact angle was recorded. The reported contact angles of each IL are an average of at least five independent measurements.

COSMO-RS calculations

The Conductor-like Screening Model for Real Solvents (COSMO-RS), developed by Klamt and co-workers,33,34 is a quantum chemical based method used for the prediction of the thermodynamic properties of pure and mixed fluids. In COSMO-RS, molecules are treated as a collection of surface segments. An expression for the chemical potential of segments in the condensed phase is derived, and in which the interaction energies between segments are calculated from COSMO-RS. The chemical potential of each molecule is then obtained by summing the contributions of the segments. The advantage of using COSMO-RS compared to other prediction methods, such as Quantitative Structure-Properties Relationship (QSPR), is that this model only requires the chemical structure information of the desired molecules, and thus can be simply used as *a priori* approach. In addition, owing to its quantum chemical-based approach, it provides a more accurate and detailed description of the electronic/molecular descriptors than empirical methods.48

In this work, the cation–anion pair interaction energies were generated using the COSMOthermX program, parameter file BP_TZVP_C20_0111 (COSMOlogic GmbH & Co KG, Leverkusen, Germany).49 All the COSMO files required are available in the COSMOthermX database. In COSMO-RS, the total IL cation–anion interaction energy (E_{INT}) arises from the sum of three specific interactions, namely electrostatic-misfit (E_{MF}), hydrogen-bond (E_{HB}), and van der Waals energies (E_{vdW}) that can be expressed as

$$E_{INT} = E_{MF} + E_{HB} + E_{vdW} \quad (7)$$

In addition to those four descriptors, we introduced an additional descriptor, namely the ring correction energy, E_{Ring}, which depends on the number of atoms which compose a given IL cation ring (see Table S1 in the ESI†).

In a previous work,28 the best predictions of the experimental data were obtained with the lowest energy conformations or with the global minimum for both the IL cation and anion. Thus, in this work, the lowest energy conformations of all species involved were used in the COSMO-RS calculations.

Supplementary Material

Refer to Web version on PubMed Central for supplementary material.

Acknowledgements

This work was developed in the scope of project CICECO – Aveiro Institute of Materials (Ref. FCT UID/CTM/50011/2013), financed by national funds through Fundação para a Ciência e a Tecnologia (FCT, Portugal)/MEC

and co-financed by FEDER under the PT2020 Partnership agreement. Thanks are also due to FCT/MEC for the financial support to the QOPNA research Unit (FCT UID/QUI/00062/2013), through national founds, co-financed by FEDER within the PT2020 Partnership Agreement. M. M. Pereira and F. L. Sousa acknowledge the financial support from Coordenação de Aperfeiçoamento de Pessoal de Nível Superior – Capes for the PhD grant (2740-13-3) and FCT for the post-doctoral grant SFRH/BPD/71033/2010, respectively. The research leading to results reported in this work has received funding from the European Research Council under the European Union's Seventh Framework Programme (FP7/2007-2013)/ERC grant agreement no. 337753.

Notes and references

1. Wasserscheid, P.; Welton, T. Ionic Liquids in Synthesis. 2nd edn. Vol. 1. Wiley-VCH Verlag GmbH & Co. KGaA; Darmstadt, Federal Republic of Germany: 2009.
2. Rogers RD. Nature. 2007; 447:917. [PubMed: 17581570]
3. Plechkova NV, Seddon KR. Chem Soc Rev. 2008; 37:123. [PubMed: 18197338]
4. An Y, Cheng X, Zuo P, Liao L, Yin G. Mater Chem Phys. 2011; 128:250.
5. Bazito FFC, Kawano Y, Torresi RM. Electrochim Acta. 2007; 52:6427.
6. Tariq M, Freire MG, Saramago B, Coutinho JAP, Lopes JNC, Rebelo LPN. Chem Soc Rev. 2012; 41:829. [PubMed: 21811714]
7. Page PM, McCarty TA, Baker GA, Baker SN, Bright FV. Langmuir. 2007; 23:843. [PubMed: 17209642]
8. Gao L, McCarthy TJ. J Am Chem Soc. 2007; 129:3804. [PubMed: 17352481]
9. Restolho J, Mata JL, Saramago B. J Colloid Interface Sci. 2009; 340:82. [PubMed: 19748101]
10. Restolho J, Mata JL, Saramago B. J Chem Phys. 2011; 134:074702. [PubMed: 21341864]
11. Restolho J, Mata JL, Saramago B. Fluid Phase Equilib. 2012; 322–323:142.
12. Restolho J, Mata JL, Shimizu K, Canongia Lopes JN, Saramago B. J Phys Chem C. 2011; 115:16116.
13. Carrera GVSM, Afonso CAM, Branco LC. J Chem Eng Data. 2010; 55:609.
14. Paneru M, Priest C, Sedev R, Ralston J. J Phys Chem C. 2010; 114:8383.
15. Millefiorini S, Tkaczyk AH, Sedev R, Efthimiadis J, Ralston J. J Am Chem Soc. 2006; 128:3098. [PubMed: 16506791]
16. Paneru M, Priest C, Ralston J, Sedev R. J Adhes Sci Technol. 2012; 26:2047.
17. Halka V, Freyland W. Zeitschrift fur Physikalische Chemie. 2008; 222:117.
18. Restolho J, Mata JL, Saramago B. J Phys Chem C. 2009; 113:9321.
19. Freire MG, Neves CMSS, Carvalho PJ, Gardas RL, Fernandes M, Marrucho IM, Santos LMNBF, Coutinho JAP. J Phys Chem B. 2007; 111:13082. [PubMed: 17958353]
20. Freire MG, Carvalho PJ, Gardas RL, Santos LMNBF, Marrucho IM, Coutinho JAP. J Chem Eng Data. 2008; 53:2378.
21. Kurnia KA, Sintra TE, Neves CMSS, Shimizu K, Canongia Lopes JN, Goncalves F, Ventura SPM, Freire MG, Santos LMNBF, Coutinho JAP. Phys Chem Chem Phys. 2014; 16:19952. [PubMed: 25119425]
22. Kurnia KA, Quental MV, Santos LB, Freire MG, Coutinho JAP. Phys Chem Chem Phys. 2015; 17:4569. [PubMed: 25583632]
23. Freire MG, Carvalho PJ, Gardas RL, Marrucho IM, Santos LMNBF, Coutinho JAP. J Phys Chem B. 2008; 112:1604. [PubMed: 18201080]
24. Freire MG, Neves CMSS, Shimizu K, Bernardes CES, Marrucho IM, Coutinho JAP, Canongia Lopes JN, Rebelo LPN. J Phys Chem B. 2010; 114:15925. [PubMed: 21077599]
25. Martins MAR, Neves CMSS, Kurnia KA, Andreia L, Santos LMNBF, Freire MG, Pinho SP, Coutinho JAP. Fluid Phase Equilib. 2014; 375:161.
26. Neves CMSS, Kurnia KA, Shimizu K, Marrucho IM, Rebelo LPN, Coutinho JAP, Freire MG, Canongia Lopes JN. Phys Chem Chem Phys. 2014; 16:21340. [PubMed: 25179181]
27. Martins MAR, Neves CMSS, Kurnia KA, Santos LMNBF, Freire MG, Pinho SP, Coutinho JAP. Fluid Phase Equilib. 2014; 381:28.

28. Cláudio AFM, Swift L, Hallett JP, Welton T, Coutinho JAP, Freire MG. Phys Chem Chem Phys. 2014; 16:6593. [PubMed: 24569531]
29. Kurnia KA, Lima F, Cláudio AFM, Coutinho JAP, Freire MG. Phys Chem Chem Phys. 2015; 17:18980. [PubMed: 26129926]
30. Kurnia KA, Pinho SP, Coutinho JAP. Green Chem. 2014; 16:3741.
31. Ferreira AR, Freire MG, Ribeiro JC, Lopes FM, Crespo JG, Coutinho JAP. Fuel. 2014; 128:314.
32. Neves CMSS, Granjo JFO, Freire MG, Robertson A, Oliveira NMC, Coutinho JAP. Green Chem. 2011; 13:1517.
33. Klamt A, Eckert F. Fluid Phase Equilib. 2000; 172:43.
34. Klamt, A. COSMO-RS from quantum chemistry to fluid phase thermodynamics and drug design. Elsevier, Amsterdam; The Netherlands: 2005.
35. Batchelor T, Cunder J, Fadeev AY. J Colloid Interface Sci. 2009; 330:415. [PubMed: 19027916]
36. Freire MG, Neves CMSS, Marrucho IM, Coutinho JAP, Fernandes AM. J Phys Chem A. 2010; 114:3744. [PubMed: 20235600]
37. Cione AM, Mazyar OA, Booth BD, McCabe C, Jennings GK. J Phys Chem C. 2009; 113:2384.
38. Ferreira R, Blesic M, Trindade J, Marrucho I, Lopes JNC, Rebelo LPN. Green Chem. 2008; 10:918.
39. Anwander R, Palm C, Groeger O, Engelhardt G. Organometallics. 1998; 17:2027.
40. Li H, Sedev R, Ralston J. Phys Chem Chem Phys. 2011; 13:3952. [PubMed: 21240433]
41. Lemus J, Neves CMSS, Marques CFC, Freire MG, Coutinho JAP, Palomar J. Environmental Sciences: Processes and Impacts. 2013; 15:1752.
42. Lemus J, Martin-Martinez M, Palomar J, Gomez-Sainero L, Gilarranz MA, Rodriguez JJ. Chem Eng J. 2012; 211-212:246.
43. Neves CMSS, Lemus J, Freire MG, Palomar J, Coutinho JAP. Chem Eng J. 2014; 252:305. [PubMed: 25516713]
44. Ab Rani MA, Brant A, Crowhurst L, Dolan A, Lui M, Hassan NH, Hallett JP, Hunt PA, Niedermeyer H, Perez-Arlandis JM, Schrems M, et al. Phys Chem Chem Phys. 2011; 13:16831. [PubMed: 21858359]
45. Palomar J, Ferro VR, Torrecilla JS, Rodríguez F. Ind Eng Chem Res. 2007; 46:6041.
46. Palomar J, Torrecilla JS, Lemus J, Ferro VR, Rodriguez F. Phys Chem Chem Phys. 2010; 12:1991. [PubMed: 20145869]
47. Ghanem OB, Mutalib M, El-Harbawi M, Gonfa G, Kait CF, Alitheen NBM, Lévêque JM. J Hazard Mater. 2015; 297:198. [PubMed: 25965417]
48. Karelson M, Lobanov VS, Katritzky AR. Chem Rev. 1996; 96:1027. [PubMed: 11848779]
49. Eckert, F.; Klamt, A. COSMOlogic GmbH & Co. KG; Leverkusen, Germany: 2006.

Europe PMC Funders Author Manuscripts

Europe PMC Funders Author Manuscripts

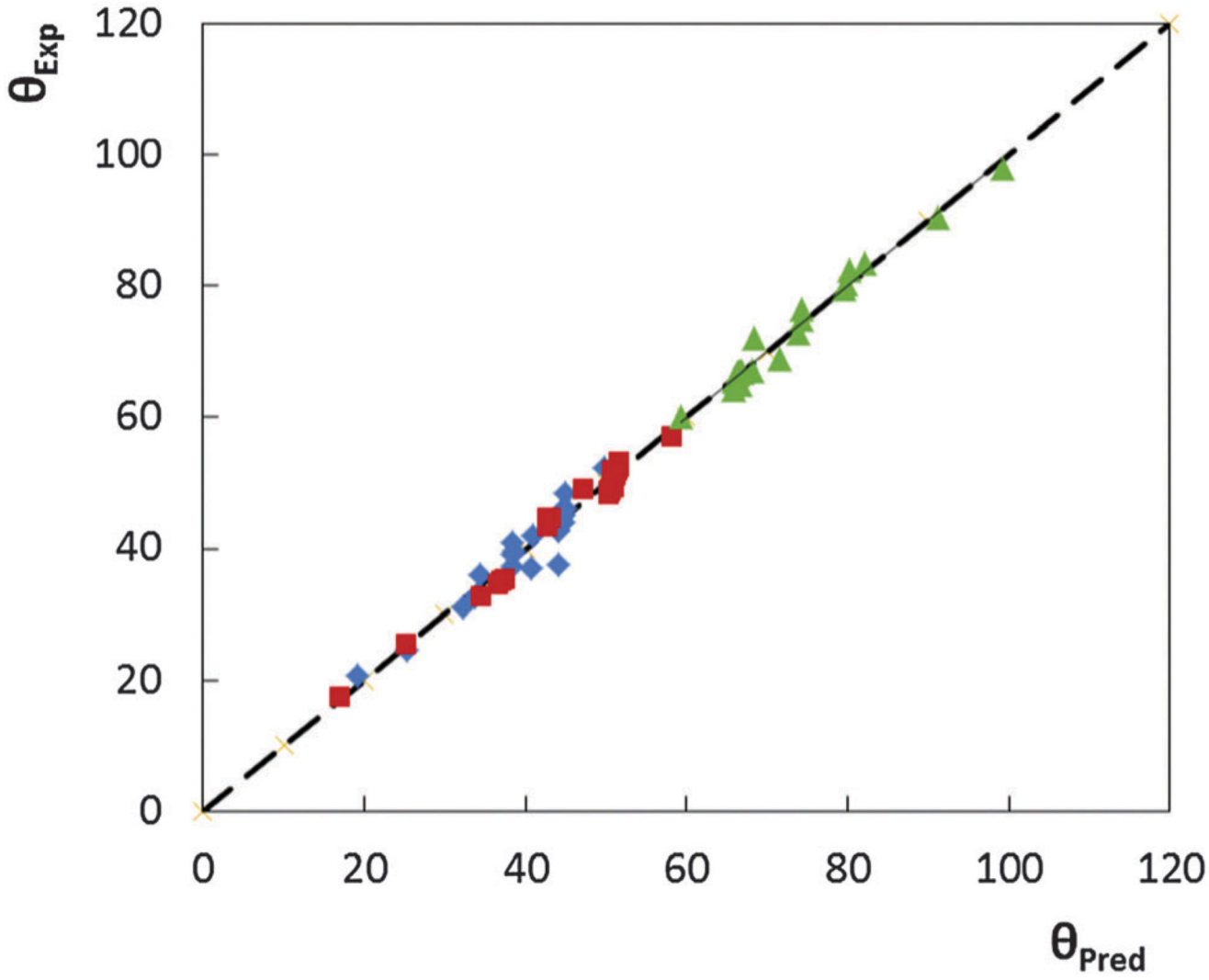

Fig. 1.

Comparison between experimental (at 298.2 K) and predicted contact angles of ILs on polar and non-polar surfaces. Symbols: (♦), glass; (■), Al-plate; and (▲), PTFE.

Europe PMC Funders Author Manuscripts

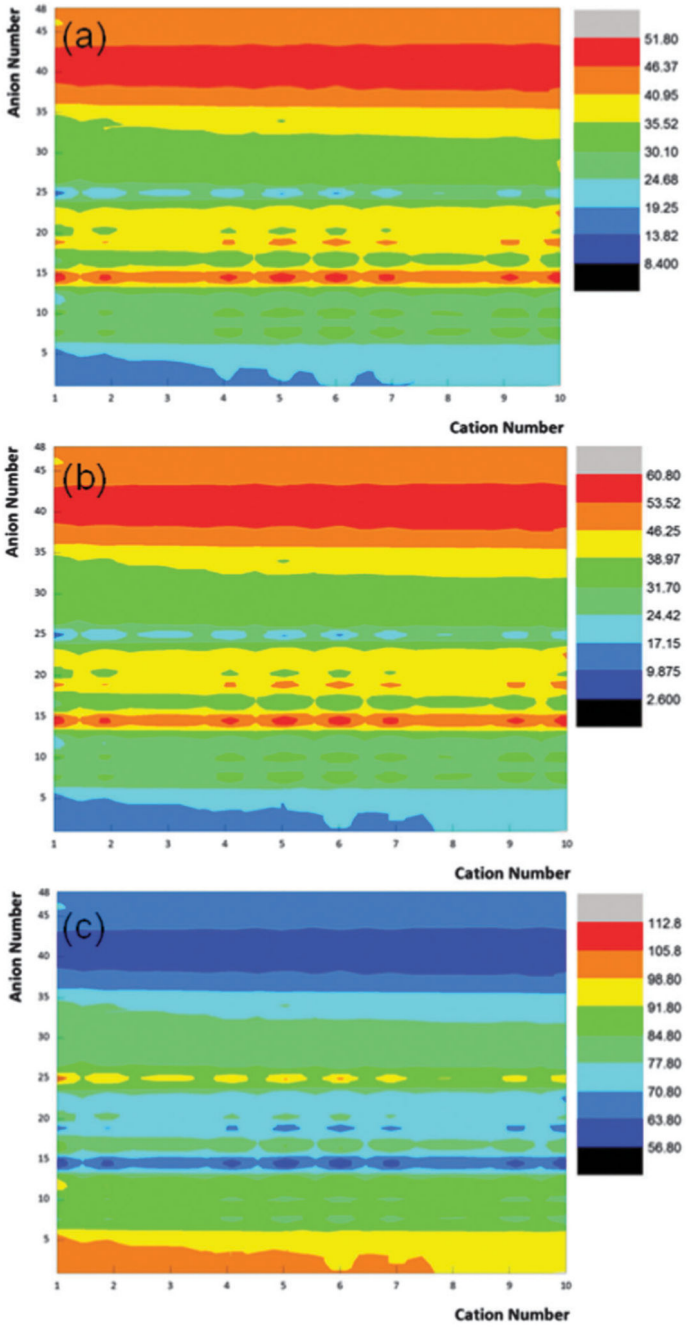

Fig. 2.
Predicted contact angles of 480 ILs on glass (a), Al-plate (b) and PTFE (c) surfaces.

Europe PMC Funders Author Manuscripts

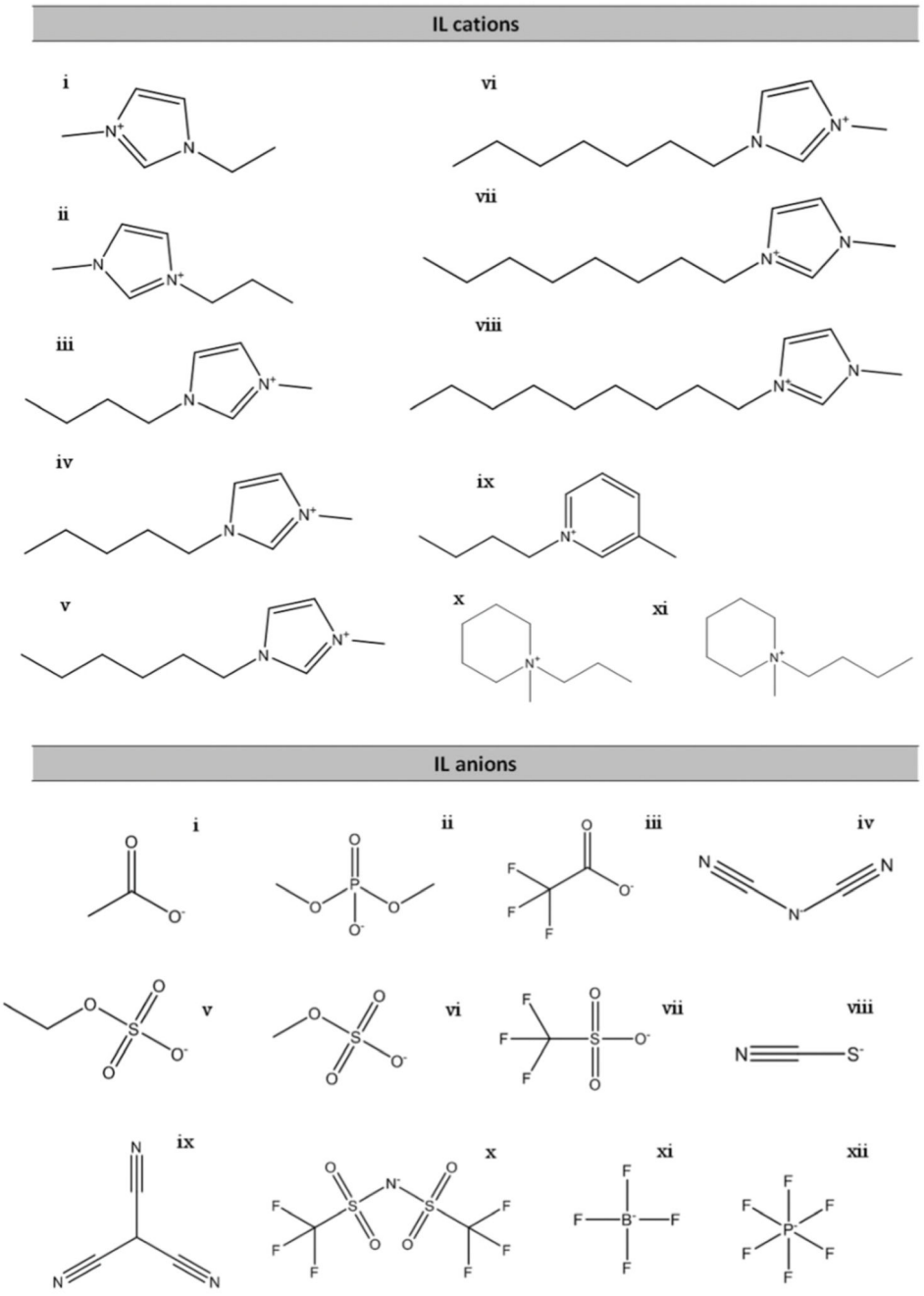

Fig. 3.

Chemical structures of cations and anions composing the studied ILs. Cations: (i) 1-ethyl-3-methylimidazolium (ii) 1-propyl-3-methylimidzolium, (iii) 1-butyl-3-methylimidazolium, (iv) 1-pentyl-3-methylimidazolium, (v) 1-hexyl-3-methylimidazolium, (vi) 1-heptyl-3-methylimidazolium, (vii) 1-octyl-3-methylimidazolium, (viii) 1-nonyl-3-methylimidazolium, (ix) 1-butyl-3-methylpyridinium, (x) 1-methyl-1-propylpiperidinium, and (xi) 1-butyl-1-methylpiperidinium. Anions: (i) acetate, (ii) dimethylphosphate, (iii) trifluoroacetate, (iv) dicyanamide, (v) ethylsulfate, (vi) methylsulfate, (vii)

trifluoromethanesulfonate, (viii) thiocyanate, (ix) tricyanomethane (x) bis(trifluoromethanesulfonyl)imide, (xi) tetrafluoroborate, and (xii) hexafluorophosphate.

Europe PMC Funders Author Manuscripts

Europe PMC Funders Author Manuscripts

Table 1

Contact angles, θ, of the ILs investigated on the polar glass and Al-plate surfaces, and on the non-polar PTFE surface, at 298.2 K, along with the respective standard deviations, σ

	($\theta \pm \sigma$)/deg		
Ionic liquids	**Glass**	**Al-plate**	**PTFE**
$[C_4C_1im][Ac]$	20.63 ± 0.03	17.67 ± 0.01	98.03 ± 0.02
$[C_4C_1im][DMP]$	24.56 ± 0.91	25.64 ± 0.17	90.48 ± 0.16
$[C_4C_1im][TFA]$	31.03 ± 0.11	32.79 ± 0.05	83.43 ± 0.36
$[C_4C_1im][N(CN)_2]$	32.54 ± 0.99	34.60 ± 0.02	82.38 ± 0.30
$[C_4C_1im][EtSO_4]$	33.25 ± 0.94	35.36 ± 0.17	80.32 ± 0.32
$[C_4C_1im][MeSO_4]$	36.11 ± 0.70	35.57 ± 0.02	79.54 ± 0.26
$[C_4C_1im][CF_3SO_3]$	37.24 ± 0.11	43.45 ± 0.88	76.43 ± 0.17
$[C_4C_1im][SCN]$	39.21 ± 0.91	44.75 ± 0.27	74.77 ± 0.19
$[C_4C_1im][C(CN)_3]$	39.57 ± 0.40	44.91 ± 0.68	72.74 ± 0.06
$[C_4C_1im][NTf_2]$	43.87 ± 0.12	49.43 ± 0.43	66.76 ± 0.06
$[C_4C_1im][BF_4]$	45.63 ± 0.50	52.13 ± 0.10	65.07 ± 0.07
$[C_4C_1im][PF_6]$	52.46 ± 0.93	57.20 ± 0.27	60.11 ± 0.07
$[C_2C_1im][NTf_2]$	37.66 ± 0.35	48.50 ± 0.21	66.93 ± 0.01
$[C_3C_1im][NTf_2]$	42.85 ± 0.05	49.01 ± 0.09	66.82 ± 0.06
$[C_5C_1im][NTf_2]$	43.96 ± 0.23	50.29 ± 0.36	66.53 ± 0.03
$[C_6C_1im][NTf_2]$	44.12 ± 0.10	51.22 ± 0.11	66.10 ± 0.38
$[C_7C_1im][NTf_2]$	45.09 ± 0.14	52.07 ± 0.02	65.95 ± 0.15
$[C_8C_1im][NTf_2]$	48.58 ± 0.23	52.60 ± 0.13	65.60 ± 0.17
$[C_9C_1im][NTf_2]$	46.11 ± 0.69	53.28 ± 0.52	64.14 ± 0.33
$[C_3C_1pip][NTf_2]$	37.02 ± 0.17	48.99 ± 0.63	71.97 ± 0.78
$[C_4C_1pip][NTf_2]$	41.99 ± 0.13	49.30 ± 0.27	67.21 ± 0.02
$[C_4C_1py][NTf_2]$	41.04 ± 0.07	49.26 ± 0.16	68.88 ± 0.80

Table 2

Correlation between the experimental contact angles of ILs on the polar SiO_2 (glass), θ_g, Al-plate, θ_{Al}, and non-polar PTFE (Teflon), θ_T, surfaces and the cation–anion interaction energies (in kJ mol^{-1}) estimated using COSMO-RS. The respective correlation coefficient, R^2, Fisher significance parameter, F, and average absolute standard deviation, AARD, are also provided

	R^2	F	AARD/%	Eqn
$\theta_G = ((0.7346 \pm 0.0730) \times E_{HB}) + (49.95 \pm 1.17)$	0.8005	101.2942	5.29	(1)
$\theta_G = ((0.8336 \pm 0.0516) \times E_{HB}) + ((10.02 \pm 1.79) \times E_{Ring}) + (91.38 \pm 7.45)$	0.9117	130.1319	3.89	(2)
$\theta_{Al} = ((1.0414 \pm 0.0554) \times E_{HB}) + (59.45 \pm 0.88)$	0.9338	353.8392	3.91	(3)
$\theta_{Al} = ((1.1201 \pm 0.0365) \times E_{HB}) + ((7.96 \pm 1.26) \times E_{Ring}) + (92.39 \pm 5.25)$	0.9746	481.8869	3.08	(4)
$\theta_T = ((-0.9855 \pm 0.0606) \times E_{HB}) + (58.45 \pm 0.96)$	0.9133	264.4063	2.68	(5)
$\theta_T = ((-1.0788 \pm 0.0333) \times E_{HB}) + ((-9.45 \pm 1.15) \times E_{Ring}) + (19.35 \pm 4.80)$	0.9769	481.8869	3.08	(6)